

Benchmarking Adversarial Patch Selection and Location

Shai Kimhi
Technion

shai.kimhi@cs.technion.ac.il

Avi Mendelson
Technion

mendlson@technion.ac.il

Moshe Kimhi
Technion

moshekimhi@cs.technion.ac.il

Abstract

*Adversarial patch attacks threaten the reliability of modern vision models. We present **PatchMap**, the first spatially exhaustive benchmark of patch placement, built by evaluating over 1.5×10^8 forward passes on ImageNet validation images. PatchMap reveals systematic “hot-spots” where small patches (as little as 2% of the image) induce confident misclassifications and large drops in model confidence. To demonstrate its utility, we propose a simple segmentation-guided placement heuristic that leverages off-the-shelf masks to identify vulnerable regions without any gradient queries. Across five architectures—including adversarially trained ResNet-50—our method boosts attack success rates by 8–13 percentage points compared to random or fixed placements. We publicly release **PatchMap**¹ and the code implementation². The full **PatchMap** bench (6.5 B predictions, multiple backbones) will be released upon acceptance to further accelerate research on location-aware defenses and adaptive attacks.*

tacks.

1. Introduction

Deep neural networks have achieved near-human accuracy on many vision benchmarks, yet they remain alarmingly brittle to small, localized perturbations. In particular, *adversarial patches*—printed stickers or posters that can be physically applied to a scene—have been shown to reliably fool classifiers and detectors in both digital and real-world settings [1, 3, 18]. Their practical threat spans self-driving cars, surveillance systems, and biometric authentication.

Despite extensive work on crafting patch *appearance*—optimizing texture, shape, and color—little attention has been paid to the equally critical question of *where* to place a patch. Most defenses and evaluation protocols implicitly assume a fixed placement (e.g. center or corner of the image) or explore joint location–texture optimization on a handful of examples [15, 21]. Without a systematic, large-scale

study of spatial vulnerability, researchers cannot reliably benchmark location-aware attacks, nor can they design defenses that guard against worst-case placements.

Motivation. Consider two identical patches: one pasted over a salient object region, the other over background. Intuitively, the former will more strongly disrupt classification, yet existing benchmarks provide only sparse evidence for this intuition. A comprehensive spatial analysis would answer: Which regions of a natural image are most susceptible? How does vulnerability vary across object classes, patch size, and model architecture? And crucially, can we exploit this knowledge to mount faster, more effective attacks without model queries?

PatchMap. We introduce *PatchMap*, the first *spatially exhaustive* benchmark for adversarial patch placement. Starting from the ten transferable patches of the ImageNet-Patch dataset [12], we paste each patch at every stride-2 location and three scale factors (50, 25, 10 px) on all 50k ImageNet-1K validation images. This yields over 1.0×10^8 forward passes on a standard ResNet-50, recording both predicted labels and softmax confidences at each location. These dense “vulnerability maps” uncover stable hot-spots, quantify confidence collapse patterns, and reveal spatial motifs invisible to prior small-scale studies.

Contributions

- PatchMap dataset.** A public release of 100 M+ location-conditioned predictions on [HuggingFace](#), scaling to 6.5 B entries.
- Rigorous analysis.** Unified definitions of attack-success rate (ASR) and confidence drop (Δconf), evaluated across location, patch size, and model robustness, exposing recurring spatial vulnerabilities.
- Segmentation-guided placement.** A fast, zero-gradient heuristic that selects high-impact locations via off-the-shelf semantic masks, boosting ASR by 8–13 pp over random or fixed baselines—even on adversarially trained networks.

By decoupling *what* a patch looks like from *where* it lands, PatchMap lays the groundwork for location-aware

¹huggingface.co/datasets/PatchMap/PatchMap_v1

²github.com/PatchMap7/PatchMap

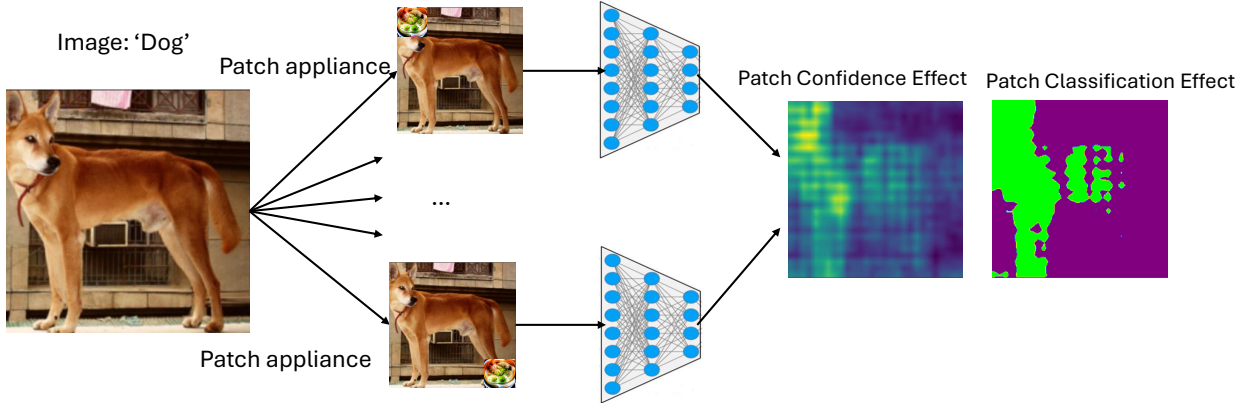


Figure 1. PatchMap evaluation method: We apply patch for any location in the image, and for each location we estimate the predicted class of the model and the confidence of the model on the ground truth class (y).

defenses, adaptive attacks, and deeper insight into the spatial dynamics of adversarial vulnerability.

2. Related Work

2.1. Universal and Physical Adversarial Patches

[1] first introduced *universal* patches that consistently coerce a classifier into an attacker-chosen label. Because these patches are *physically realizable*, later studies printed them to fool real-world systems: LaVAN places a small visible blob on the background [6], while RP2 stickers make stop-signs read as speed-limits [3]. Domain-specific variants exist for face recognition, where perturbations are embedded in eyeglass frames [18], and for traffic-sign detection [20]. The feasibility of such localised, robust attacks motivated datasets such as ImageNet-Patch [12], which supplies transferable patch textures later reused in our work.

2.2. Patch Placement and Location Optimisation

Early attacks fixed the patch at a predetermined corner or the object centre [3, 6], implicitly assuming position mattered little. Subsequent research relaxed this by *optimising* location jointly with texture: LOAP employs gradient descent on both variables [15]; Simultaneous-Patch uses reinforcement learning (RL) to search position in a black-box setting [21]; PatchAttack learns an RL policy subject to a query budget [24]. Real-world “Adversarial Sticker” work further optimises in-plane rotation and scale of printed patches [22]. Generative Dynamic Patch Attack (GDPA) [11] uses GANs to propose both content and location, showing that placement is tightly coupled with texture generation. Attention-guided methods such as PS-GAN

[13] infer high-impact regions from saliency maps, while Shapeshifter extends the idea to object detection [3]. Despite this progress, prior studies either optimise on a handful of images or evaluate sparse locations; none offers an *exhaustive*, publicly released map of spatial vulnerability.

2.3. Context Awareness and Adaptive Attacks

Modern attacks adapt the patch to scene context. Distributed stickers cover multiple object parts for occlusion robustness [22], and Dynamic-Patch sequences adjust appearance over time [11]. Beyond classification, context-aware patches fool detectors, depth estimators, and segmentation networks, often by incorporating physical transforms (viewpoint, lighting) into training [3]. Several works exploit semantic priors: masking patches to background only, or using segmentation cues to stay off salient regions [14]. Our segmentation-guided heuristic takes the opposite tack—*seeking* the most segmentation-confident region—while remaining optimisation-free and substantially faster than RL or gradient-based search.

PatchMap complements the above literature by offering the first large-scale, architecture-agnostic benchmark that *decouples* patch appearance from exhaustive placement, enabling quantitative comparison of any optimisation-free or optimisation-based strategy on common ground.

3. Dataset Design

Patch source. We use the ten publicly released ImageNet-Patch adversaries of Li et al. [12]. Each 50×50 RGB patch is gradient-optimised for a distinct target class and shown to transfer across common CNN backbones. Fixing this set

guarantees strict reproducibility and avoids the confound of re-optimising patch content. The patches are applied without rotation.

Spatial sweep. For every ImageNet-1K validation image (224×224), each patch is pasted on a dense stride-2 grid of feasible centres. The grid contains $112 \times 112 = 12,544$ positions and is evaluated at three square sizes: native 50×50 , down-scaled 25×25 , and 10×10 px covering almost the whole image while keeping compute tractable. In total $50,000$ images $\times 10$ patches $\times 3$ sizes $\times 12,544$ locations $\approx 1.9 \times 10^{10}$ potential placements. By batching inference and discarding placements that would fall outside the frame, we actually run 1.1×10^8 forward passes—roughly two orders of magnitude more than any previous location study.

Model attacked. All placements are evaluated on a standard ResNet-50 [5] from `torchvision`, pretrained on ImageNet and *not* adversarially fine-tuned. Future PatchMap releases will incorporate additional backbones, but v1.0 deliberately fixes a single architecture to keep the file size manageable.

Recorded data format. PatchMap is *sharded*: every triple (image_id, patch_id, patch_size) is stored in its `.npy` file named `{img}-{patch}-{size}.npz`. Each file contains a single NumPy array of shape $2 \times 112 \times 112$: the first slice holds the predicted class indices (`int16`); the second holds the corresponding soft-max confidences (`float32`). With 50,000 images, ten patches and three sizes, v1.0 comprises 1.5 million files totalling ~ 1.5 GB after compression. This fine-grained layout lets users download only the subsets they need and stream batches directly from disk without monolithic archives.

Resources. All benchmark evaluations can be performed with a single processor with at least 8GB of memory (with/without GPU).

Public release. PatchMap v1.0 (≈ 100 M predictions) is hosted on [HuggingFace](#) under a CC-BY-4.0 license, bundled with loaders, plotting utilities, and a leaderboard script. A 6.5 B-entry v2.0, computed on a dedicated GPU cluster, will be released under the same terms. The code implementation of the project is available on [GitHub](#) **Why PatchMap?** Its exhaustive spatial cover-

age allows researchers to *map* vulnerability hot-spots, train location-aware detectors, and benchmark optimisation-free or optimisation-based placement strategies under identical conditions.

4. Evaluation Protocol

PatchMap’s dense annotations enable four complementary evaluations.

1. **Location-wise attack-success heat-maps.** For every grid cell (r, c) we compute the *clean-correct* attack-success rate

$$\text{ASR}(r, c) = \frac{1}{N_{\text{cc}}} \sum_{i=1}^{N_{\text{cc}}} [\hat{y}_{i,r,c} \neq y_i],$$

where N_{cc} is the number of validation images that the model classifies correctly without a patch. The resulting 112×112 heat-map exposes systematic hot- and cold-spots.

2. **Confidence and calibration shift.** Besides logits, PatchMap records soft-max scores, enabling reliability analysis. We report (i) the average confidence drop Δ_{conf} as detailed in 2 and (ii) the change in Expected Calibration Error (ECE) and Brier score between clean and patched images.
3. **Size / conspicuity trade-off.** Plotting ASR against patch area across the three sizes yields a Pareto curve that answers: How small can a patch be before its success drops below a chosen threshold?
4. **Cross-model transfer.** Given placements evaluated on model A , we re-score the exact locations on model B and assemble a transfer matrix $T_{A \rightarrow B}$. Off-diagonal strength indicates universal spatial vulnerabilities; weak transfer suggests architecture-specific quirks.

Reporting. Metrics are averaged over the full validation set and accompanied by 95% bootstrap confidence intervals (1 000 resamples). The public code reproduces every figure and table in under 2 GPU-hours on a single V100.

PatchMap therefore enables fine-grained, statistically sound evaluation of both attacks and defences, opening the door to location-aware robustness research.

5. Analysis and Findings

5.1. Attack-success rate (ASR)

For every image x_i that the clean model classifies correctly, and for every patch location (k, ℓ) , let $\tilde{y}_{i,k,\ell}$ denote the predicted label on the patched image $x_i \oplus M_{k,\ell}$ and \hat{y}_i the clean prediction. The *location-wise* ASR is then

$$\text{ASR}(k, \ell) = \frac{1}{N_{\text{cc}}} \sum_{i=1}^{N_{\text{cc}}} [\tilde{y}_{i,k,\ell} \neq \hat{y}_i],$$

where N_{cc} is the number of *clean-correct* images.

Optimal location. For each image we also record the highest ASR over all positions; Table 1 reports the mean of this value across the dataset.

Table 1. Mean *optimal* ASR: fraction of images for which *some* location causes misclassification.

Patch size	Patch 2 (“Plate”)	Patch 6 (“Guitar”)
50×50	0.84	0.94
25×25	0.79	0.82
10×10	0.69	0.71

ASR_q. Let w, h be the grid dimensions (112×112). ASR in quantile q measures the proportion of images fooled at *at least* a fraction q of locations,

$$\text{ASR}_q = \frac{1}{N_{\text{cc}}} \sum_{i=1}^{N_{\text{cc}}} \mathbb{I}\left(\frac{1}{wh} \sum_{k=1}^w \sum_{\ell=1}^h [\tilde{y}_{i,k,\ell} \neq \hat{y}_i] > q\right). \quad (1)$$

Figure 2 plots ASR_q for two representative patches.

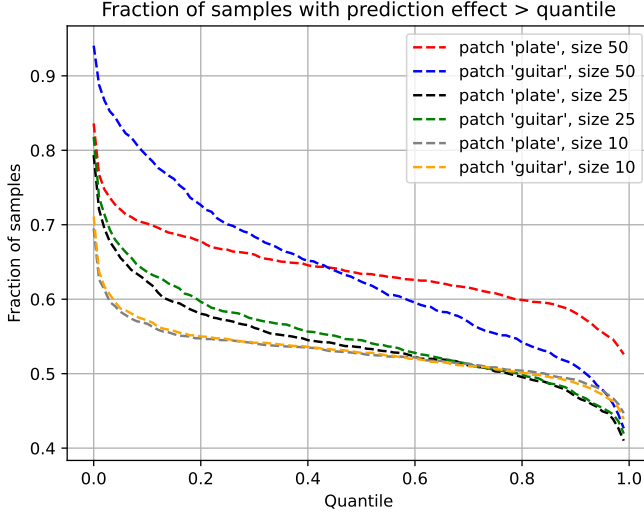


Figure 2. ASR_q (1): fraction of images misclassified at more than a q -portion of locations.

ASR_q indicates the robustness of the effect of the patch on the model with respect to the location of the patch in the image. Patch “Plate” of size 50×50 is the most robust in that sense, as effect is least effected by location obtaining the best results for the worst $\approx 60\%$ of patch locations, “Guitar” of size 50×50 obtains the best results for $\approx 40\%$ of the best patch locations.

5.2. Confidence effect

Let $p_{\theta}(y_i \mid x_i)$ be the clean soft-max confidence of the ground-truth class y_i . The *confidence drop* for image i is

$$\Delta\text{conf}_i = \max_{k,\ell} [p_{\theta}(y_i \mid x_i) - p_{\theta}(y_i \mid x_i \oplus M_{k,\ell})], \quad (2)$$

i.e. the largest fall among all locations. Table 2 shows the mean Δconf per patch size.

Table 2. Average confidence drop (Δconf) at the worst location per image.

Patch size	Patch 2	Patch 6
50×50	0.62	0.71
25×25	0.60	0.62
10×10	0.45	0.48

Figure 3 plots the distribution of post-attack confidences; larger patches incur heavier tails towards low confidence, with the “Guitar” patch producing the sharpest degradation at 50×50 .

6. Segmentation-Guided Patch Placement

6.1. Motivation

Most patch attacks search location by gradient descent or reinforcement learning-effective but slow and model-dependent. We observe that semantic-segmentation networks already highlight the pixels most critical for recognizing objects. If a patch occludes those pixels, it should hurt the classifier without any extra optimization. We therefore use segmentation confidence as a *fast, architecture-agnostic* cue for placing the patch, that proven to be valid when trained on sufficient amount of data [9], despite their limitations [8].

6.2. Approach

Let $g(x) \in [0, 1]^{H \times W \times C}$ be per-pixel soft-max scores from a segmentation model, where channel b is *background*. Define the object-confidence map

$$S = 1 - g(x)_b.$$

Given a binary patch mask $M \in \{0, 1\}^{s \times s}$, we slide M over S and pick the location that maximises the summed confidence it covers:

$$(k^*, \ell^*) = \arg \max_{k,\ell} (S \odot \text{Shift}_{k,\ell}(M))_1, \quad (3)$$

where \odot is the element-wise product, $\text{Shift}_{k,\ell}$ centres the mask at (k, ℓ) , and $(\cdot)_1$ sums all entries. The chosen centre (k^*, ℓ^*) is used for every tested classifier; no gradients or queries to the attacked model are required.

6.3. Experimental Setup

We evaluate all placement strategies on the **ImageNet-1K** validation split, resizing each image to 224×224 pixels. Five classifiers are attacked: ResNet-18 ([5]), ResNet-50, MobileNet-V2 ([17]), EfficientNet-B1 ([19]), and a Fast Adversarially Trained ResNet-50 [23]. Patch placement

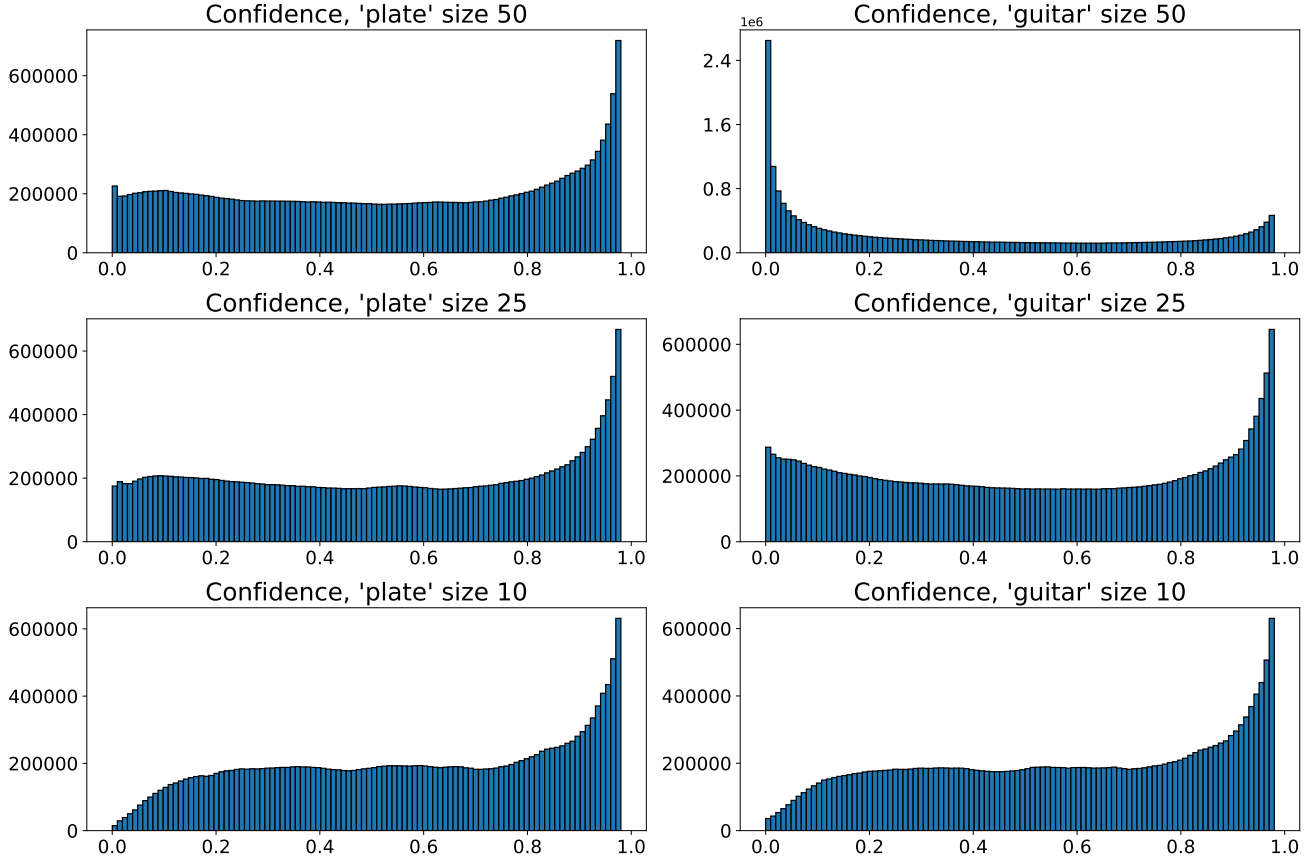


Figure 3. Histogram of soft-max confidence on the ground-truth class after patching.

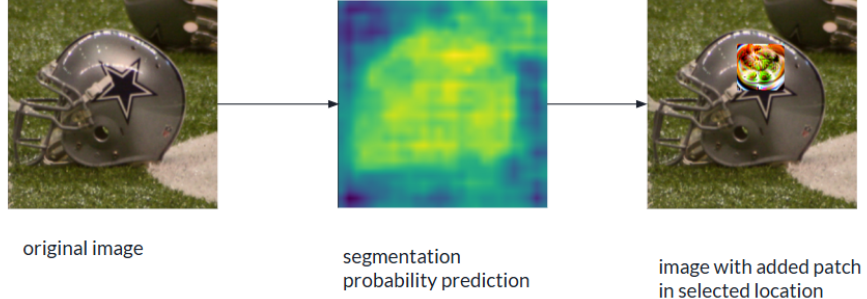


Figure 4. Pipeline of the segmentation-guided placement. A segmentation heat-map (middle) guides the patch (right) to the most confident object region.

is guided by **DeepLab-v3+**([2]) with a ResNet-101 backbone, pretrained on PASCAL-VOC 2012, whose segmentation confidences serve as a zero-gradient cue. All experiments can be conducted with a single processor with at least 8GB of memory (with/without GPU).

Unless stated otherwise, the adversary is the “Plate“ universal patch from ImageNet-Patch [12], resized to 50×50 ($\approx 4.98\%$ of the image) and without rotation. We bench-

mark three optimisation-free placement rules: (i) *Random*-uniformly sampling the patch centre, (ii) *Fixed*-choosing the best of four preset offsets from the image centre, and (iii) our *Seg-guided* heuristic described in 3.

Performance is reported as **attack-success rate (ASR)** on the subset of images that each model classifies correctly in the clean setting.

6.3.1. Results

Overall performance. Table 3 compares attack-success rates (ASR) for three optimisation-free placement strategies. Across all four ImageNet-trained architectures, the segmentation-guided (Seg-guided) heuristic achieves the highest ASR, improving on *Random* placement by an average of 8 pp and outperforming the *Fixed* four-offset baseline by 13 pp. Crucially, the advantage persists on the adversarially trained ResNet-50, where Seg-guided placement still raises ASR from 0.31–0.36 to 0.39, underscoring that robust training alone is not sufficient to counter strategic patch positioning.

Effect of patch size. Figures 6, 7 and 8 plots ASR against patch side length on a representative ResNet-18 for lengths $\{5, 15, 25, 50\}$. All methods degrade as the patch shrinks, yet Seg-guided placement maintains a consistent margin: with a 10×10 px patch-covering barely 2 % of the image-it still fools 27 % of clean-correct samples, versus 18 % for Random and 14 % for Fixed. This resilience indicates that the segmentation heat-map is a reliable cue even when the patch is almost imperceptible.

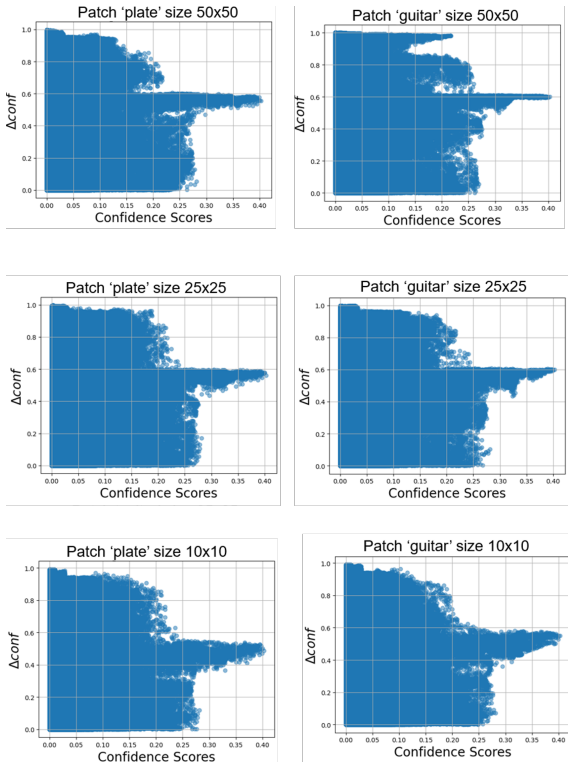


Figure 5. Correlation between segmentation confidence and classifier confidence drop (Δconf).

Table 3. ASR (\uparrow) of optimisation-free placement strategies. Patch resized with no rotation.

Model	Random	Fixed	Seg-guided
“Plate“	50×50		($\approx 4.98\%$)
ResNet-50	0.39	0.32	0.46
+ Adversarial Training [23]	0.36	0.31	0.39
ResNet-18	0.57	0.46	0.63
MobileNet-V2	0.48	0.41	0.55
EfficientNet-B1	0.37	0.35	0.43
“Plate“	25×25		($\approx 1.25\%$)
ResNet-50	0.19	0.15	0.21
+ Adversarial Training [23]	0.11	0.9	0.14
ResNet-18	0.22	0.25	0.29
MobileNet-V2	0.35	0.32	0.37
“Electric Guitar“	50×50		($\approx 4.98\%$)
ResNet-50	0.32	0.27	0.36
+ Adversarial Training [23]	0.24	0.17	0.3
ResNet-18	0.44	0.37	0.49
MobileNet-V2	0.48	0.42	0.52
“Electric Guitar“	25×25		($\approx 1.25\%$)
ResNet-50	0.19	0.16	0.22
+ Adversarial Training [23]	0.09	0.07	0.12
ResNet-18	0.25	0.22	0.28
MobileNet-V2	0.33	0.31	0.36
“Typewriter Keyboard“	50×50		($\approx 4.98\%$)
ResNet-50	0.33	0.28	0.37
+ Adversarial Training [23]	0.21	0.14	0.26
ResNet-18	0.43	0.37	0.48
MobileNet-V2	0.47	0.42	0.52
“Typewriter Keyboard“	25×25		($\approx 1.25\%$)
ResNet-50	0.18	0.15	0.20
+ Adversarial Training [23]	0.1	0.07	0.12
ResNet-18	0.23	0.19	0.25
MobileNet-V2	0.33	0.31	0.35

6.4. Correlation with Confidence Drop

We examine how segmentation confidence predicts the eventual confidence drop of the classifier at each location. Define overall object confidence

$$p_{\text{seg}}(\text{object} \mid x) = 1 - g(x)_b \quad (4)$$

(cf. Eq. 4). Figure 5 examines the correlation between segmentation confidence (as detailed previously) and the effect on the ground-truth class confidence Δconf for several possible patches. There is a strong correlation for scores

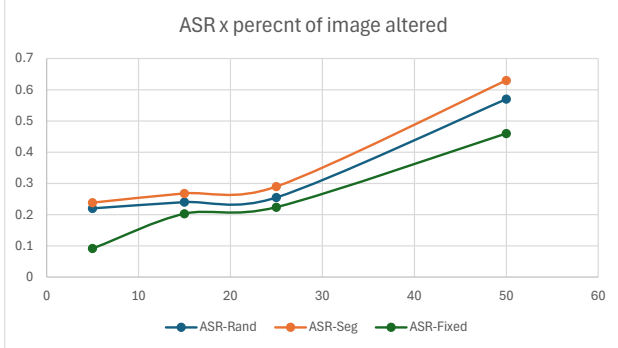


Figure 6. ASR on ResNet-18 versus patch size for patch ‘Plate’.



Figure 7. ASR on ResNet-18 versus patch size for patch ‘Type-writer’.

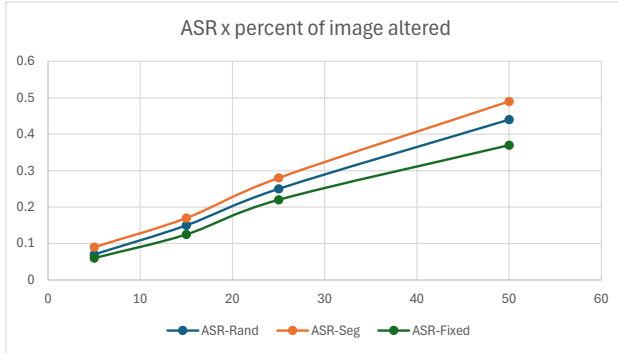


Figure 8. ASR on ResNet-18 versus patch size for patch ‘Electric Guitar’. Optimal placement remains crucial as size shrinks.

above 0.2, especially for smaller patches, confirming that the segmentation map is a useful but not perfect proxy for the worst-case location.

6.5. Qualitative Examples

Figure 9 demonstrates the connection between the segmentation probability prediction by DeepLabV3Plus with a Resnet-101 backbone as detailed in 6.3 as not object (i.e. $1 - P_\theta(class_0)$ where $class_0$ is background), and the empirical map of $\Delta conf_y$ i.e. the effect on the prediction prob-

ability of the ground-truth class y measured on ResNet-18, after appliance of patch “Plate” of size 50×50 . Most locations which yield the highest effect are indeed part of the predicted object, much of the predicted object is does not yield the highest $\Delta conf$ values.

7. Conclusion

We have introduced **PatchMap**, the first large-scale, spatially exhaustive benchmark for adversarial patch placement. By evaluating over 1.0×10^8 patch placements on ImageNet-1K validation images, PatchMap uncovers consistent “hot-spots” of vulnerability and quantifies how attack success and confidence collapse vary across both location and patch size.

Building on this dataset, we proposed a simple, **segmentation-guided placement** heuristic that leverages off-the-shelf semantic masks to select high-impact regions without any gradient queries or fine-tuning of the target model. Across five architectures—including adversarially trained ResNet-50-our method yields an 8–13 pp improvement in attack-success rate over random or fixed baselines, demonstrating that zero-gradient spatial cues can substantially amplify patch efficacy.

Looking forward, PatchMap opens the door to a new class of *location-aware* defenses and attacks, allowing for methods to find the optimal patch location with respect to universal patch attack, in new domains such as medical [16] or robotics [10]. Other direction is to understand the relation between input patch attacks and bit-flip attacks [4], as those are the most practical in real world setup.

Future releases (v2.0) will scale to 6.5 billion placements and incorporate diverse backbones (ViT, ConvNeXt and modified architectures [7]), enabling cross-family transfer studies. We anticipate that researchers will build on PatchMap to design spatially informed detectors, robust training curricula, and context-dependent attacks across classification, detection, and beyond, advancing the security and reliability of vision systems.

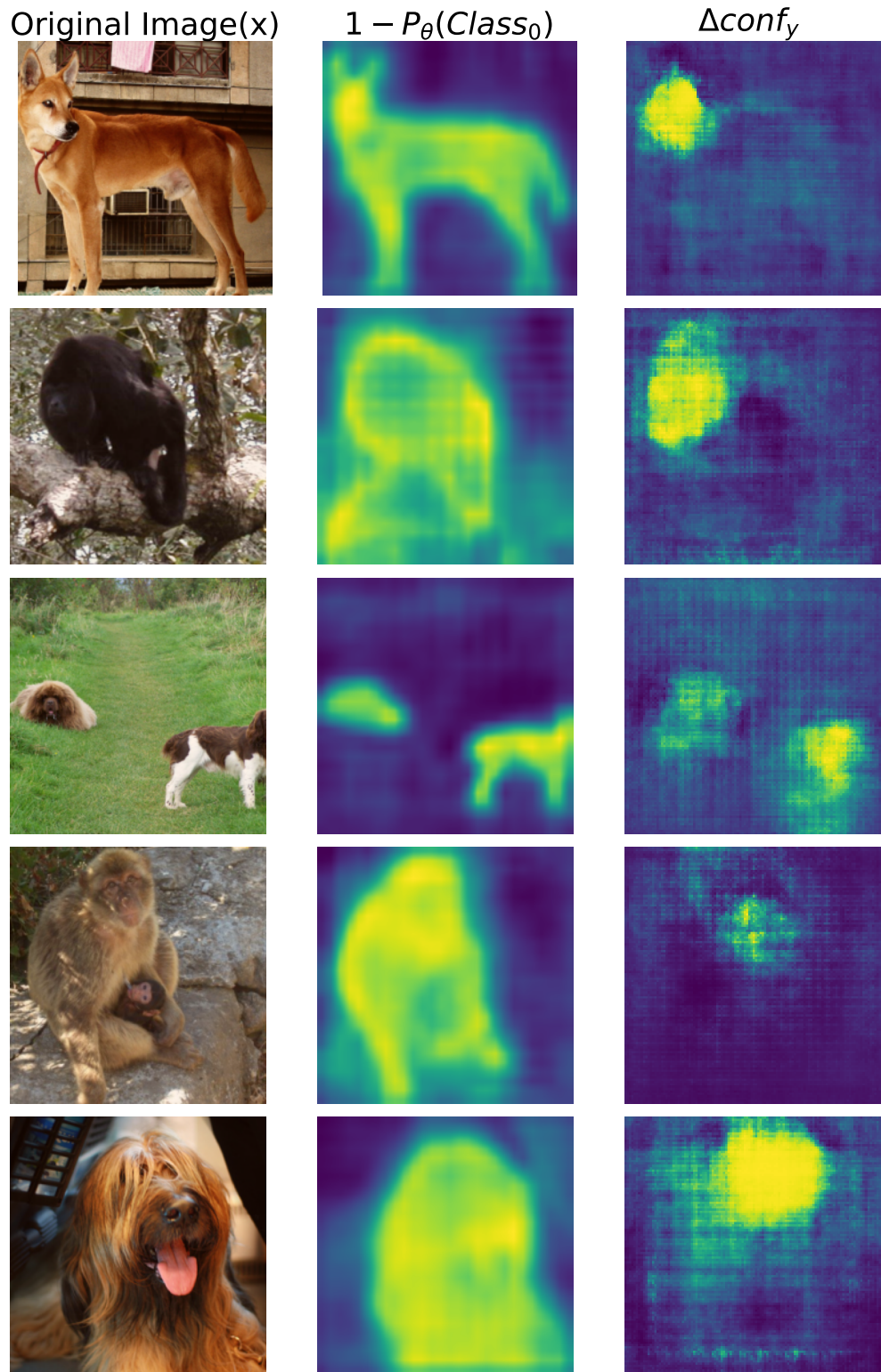


Figure 9. Left to Right: Original Image, Segmentation confidence prediction, Predicted confidence drop map, each pixel represents the confidence when the adversarial patch is applied at that location.

References

[1] Tom B. Brown, Dandelion Mane, Aurko Roy, Martin Abadi, and Justin Gilmer. Adversarial patch. *arXiv preprint arXiv:1712.09665*, 2017. [1](#), [2](#)

[2] Liang-Chieh Chen, Yukun Zhu, George Papandreou, Florian Schroff, and Hartwig Adam. Encoder-decoder with atrous separable convolution for semantic image segmentation. In *Computer Vision – ECCV 2018*, volume 11211 of *Lecture Notes in Computer Science*, pages 833–851. Springer, 2018. doi: 10.1007/978-3-030-01234-2_49. [5](#)

[3] Kevin Eykholt, Ivan Evtimov, Earlene Fernandes, Bo Li, Amir Rahmati, Chaowei Xiao, Atul Prakash, Tadayoshi Kohno, and Dawn Song. Robust physical-world attacks on deep learning visual classification. In *Proceedings of the IEEE Conference on Computer Vision and Pattern Recognition (CVPR)*, pages 1625–1634, 2018. [1](#), [2](#)

[4] Ido Galil, Moshe Kimhi, and Ran El-Yaniv. No data, no optimization: A lightweight method to disrupt neural networks with sign-flips. *arXiv preprint arXiv:2502.07408*, 2025. [7](#)

[5] Kaiming He, Xiangyu Zhang, Shaoqing Ren, and Jian Sun. Deep residual learning for image recognition, 2015. [3](#), [4](#)

[6] Danny Karmon, Daniel Zoran, and Yoav Goldberg. Lavan: Localized and visible adversarial noise. In Jennifer Dy and Andreas Krause, editors, *Proceedings of the 35th International Conference on Machine Learning (ICML)*, volume 80, pages 2507–2515. PMLR, 2018. [2](#)

[7] Moshe Kimhi, Idan Kashani, Avi Mendelson, and Chaim Baskin. Hysteresis activation function for efficient inference. In *The 4th NeurIPS Efficient Natural Language and Speech Processing Workshop*, 2024. [7](#)

[8] Moshe Kimhi, Omer Kerem, Eden Grad, Ehud Rivlin, and Chaim Baskin. Noisy annotations in semantic segmentation. *arXiv preprint arXiv:2406.10891*, 2024. [4](#)

[9] Moshe Kimhi, Shai Kimhi, Evgenii Zheltonozhskii, Or Litany, and Chaim Baskin. Semi-supervised semantic segmentation via marginal contextual information. *Transactions on Machine Learning Research*, 2024, 2024. [4](#)

[10] Moshe Kimhi, David Vainshtein, Chaim Baskin, and Dotan Di Castro. Robot instance segmentation with few annotations for grasping. In *2025 IEEE/CVF Winter Conference on Applications of Computer Vision (WACV)*, pages 7939–7949. IEEE, 2025. [7](#)

[11] Xiang Li and Shihao Ji. Generative dynamic patch attack. In *British Machine Vision Conference (BMVC)*, 2021. [2](#)

[12] Xuefei Li, Xiangyu Yin, Shiyu Chuang, Laurens van der Maaten, Raia Hadsell, and Christoph Feichtenhofer. Imagenet-patch: A dataset for benchmarking adversarial patch robustness in image classification. *arXiv preprint arXiv:2205.08649*, 2022. [1](#), [2](#), [5](#)

[13] Azadeh Liu, Xiaoyu Liu, Jun Fan, Yinpeng Ma, Aming Zhang, Heyun Xie, and Dacheng Tao. Perceptual-sensitive gan for generating adversarial patches. In *Proceedings of the AAAI Conference on Artificial Intelligence*, 2019. [2](#)

[14] Jinqi Luo, Tao Bai, and Jun Zhao. Generating adversarial yet inconspicuous patches with a single image. In *Proceedings of the Thirty-Fifth AAAI Conference on Artificial Intelligence (AAAI-21) Student Abstract and Poster Program*, pages 15837–15838, Virtual Event, 2021. doi: 10.1609/aaai.v35i18.17915. [2](#)

[15] Sai Rao, David Stutz, and Bernt Schiele. Adversarial training against location-optimized adversarial patches. In *European Conference on Computer Vision (ECCV) Workshops*, 2020. [1](#), [2](#)

[16] Olaf Ronneberger, Philipp Fischer, and Thomas Brox. U-net: Convolutional networks for biomedical image segmentation, 2015. [7](#)

[17] Mark Sandler, Andrew Howard, Menglong Zhu, Andrey Zhmoginov, and Liang-Chieh Chen. Mobilenetv2: Inverted residuals and linear bottlenecks. In *Proceedings of the IEEE/CVF Conference on Computer Vision and Pattern Recognition (CVPR)*, pages 4510–4520, 2018. doi: 10.1109/CVPR.2018.00474. [4](#)

[18] Mahmood Sharif, Sruti Bhagavatula, Lujo Bauer, and Michael K. Reiter. Accessorize to a crime: Real and stealthy attacks on state-of-the-art face recognition. In *Proceedings of the ACM Conference on Computer and Communications Security (CCS)*, pages 1528–1540. ACM, 2016. [1](#), [2](#)

[19] Mingxing Tan and Quoc V. Le. Efficientnet: Rethinking model scaling for convolutional neural networks. In *Proceedings of the 36th International Conference on Machine Learning*, volume 97 of *Proceedings of Machine Learning Research*, pages 6105–6114, 2019. URL <https://proceedings.mlr.press/v97/tan19a.html>. [4](#)

[20] Go Tsuruoka, Takami Sato, Qi Alfred Chen, Kazuki Nomoto, Ryunosuke Kobayashi, Yuna Tanaka, and Tatsuya Mori. Adversarial retroreflective patches: A novel stealthy attack on traffic sign recognition at night. In *VehicleSec 2024: Symposium on Vehicle Security and Privacy (Poster/WIP)*, pages –, San Diego, CA, USA, February 2024. doi: 10.14722/vehiclesec.2024.23025. [2](#)

[21] Xingxing Wei, Ying Guo, Jie Yu, and Bo Zhang. Simultaneously optimizing perturbations and positions for black-box adversarial patch attacks. *IEEE Transactions on Pattern Analysis and Machine Intelligence*, 2022. To appear. [1](#), [2](#)

[22] Xingxing Wei, Ying Guo, and Jie Yu. Adversarial sticker: A stealthy attack method in the physical world. *IEEE Transactions on Pattern Analysis and Machine Intelligence*, 45(3): 2711–2725, 2023. [2](#)

[23] Eric Wong, Logan Rice, and J Zico Kolter. Fast is better than free: Revisiting adversarial training. In *International Conference on Learning Representations (ICLR)*, 2020. URL <https://openreview.net/forum?id=BJx040EFvH>. [4](#), [6](#)

[24] Chenglin Yang, Adam Kortylewski, Cihang Xie, Yinzh Cao, and Alan Yuille. Patchattack: A black-box texture-based attack with reinforcement learning. In *Proceedings of the European Conference on Computer Vision (ECCV)*, 2020. [2](#)